Cerebral Cortex, 2017; 1–8

doi: 10.1093/cercor/bhx271
Original Article

ORIGINAL ARTICLE

Critical Language Areas Show Increased Functional Connectivity in Human Cortex

John D. Rolston[1] and Edward F. Chang[2]

[1]Department of Neurosurgery, University of Utah, Salt Lake City, UT 84132, USA and [2]Department of Neurological Surgery, University of California, San Francisco, CA 94143, USA

Address correspondence to Edward F. Chang, Department of Neurological Surgery, University of California, 505 Parnassus Ave., M779, San Francisco, CA 94143, USA. Email: edward.chang@ucsf.edu

Abstract

Electrocortical stimulation (ECS) mapping is routinely used to identify critical language sites before resective neurosurgery. The precise locations of these sites are highly variable across patients, occurring in the frontal, temporal, and parietal lobes—it is this variability that necessitates individual patient mapping. But why these particular anatomical sites are so privileged in each patient is unknown. We hypothesized that critical language sites have greater functional connectivity with nearby cortex than sites without critical functions, since they serve as central nodes within the language network. Functional connectivity across language, motor, and cleared sites was measured in 15 patients undergoing electrocortiographic (ECoG) mapping for epilepsy surgery. Critical language sites had significantly higher connectivity than sites without critical functions ($P = 0.001$), and this also held for motor sites ($P = 0.022$). These data support the hypothesis that critical language sites are highly connected within the local cortical network, perhaps explaining why their disruption with ECS leads to transient disturbances in language function. It is our hope that improved understanding of the mechanisms of ECS will permit improved surgical planning and perhaps contribute to the understanding of normal language physiology.

Key words: alpha band, electrical stimulation, electrocorticography, mapping, speech

Introduction

Electrocortical stimulation (ECS) is a standard clinical tool for localizing critical language function in patients undergoing neurosurgical procedures (Penfield and Erickson 1941; Penfield and Jasper 1954; Ojemann et al. 1989; Ojemann 1991, 1993). ECS can produce selective transient deficits during language tasks like naming, repetition, and counting (Penfield and Erickson 1941; Penfield and Jasper 1954; Berger et al. 1989; Sanai et al. 2008). This localization is used to make important decisions about brain regions that can be safely resected during surgery—areas where ECS produces deficits are labeled as critical language regions. To protect their presumed function, a margin of tissue is preserved around these "eloquent" areas during surgical resection for indications like tumors or epilepsy.

Yet despite the routine use of ECS in neurosurgery after its introduction by Penfield 70 years ago, the mechanisms of electrical stimulation-based disruption of language function remain unclear. Critical sites are highly variable in location across patients, and have been identified in the frontal, temporal, and parietal lobes (Ojemann et al. 1989; Chang et al. 2017). Indeed, this variability is why ECS is so crucial for surgical planning, since function and anatomy are not reliably correlated. Furthermore, ECS of highly focal areas, as discrete as 1–2 cm^2, will cause disruption of relatively complex language functions such as confrontational picture naming. In contrast, both non-invasive functional imaging and intracranial physiological recordings have yielded a radically different representation of language localization that involves far greater spatial activation of peri-sylvian cortical networks (Ojemann et al. 1989; Ojemann 1991, 2013; Swanson et al. 2007; Findlay et al. 2012; Herman et al. 2013). Why specific discrete sites within language networks induce a transient language deficit, and others do not, is an outstanding question.

We hypothesized that critical language sites feature greater connectivity with surrounding cortex, as compared to sites not identified as critical language areas by ECS. The heightened connectivity of critical language sites allows focal stimulation to more easily spread, triggering responses in a greater volume of tissue, and thereby making disruption of distributed language networks more likely.

In this paper, we tested our hypothesis by examining resting-state functional connectivity in epilepsy patients undergoing electrocorticographic (ECoG) mapping prior to epilepsy surgery (Yang et al. 2014). Metrics of functional connectivity relate correlated changes in neural activity to estimates of indirect or direct influence of one region on another, and multiple techniques exist for their calculation (Foster et al. 2016). Of the many available methods, we chose to use a metric called imaginary coherence. The omission of the real part of coherence negates spurious correlations with zero time lag (e.g., from volume conduction or common references), thereby providing a more conservative metric of connectivity in imaginary coherence than other methods (Nolte et al. 2004; Guggisberg et al. 2008).

Materials and Methods

Subjects

Fifteen patients undergoing elective left-sided extraoperative electrocorticography (ECoG) for seizure focus mapping were recruited to participate, along with 4 right-sided ECoG patients. The study was approved by the University of California, San Francisco, institutional review board (CHR #10-03 842) and all patients gave informed consent for both the surgery and, separately, the research study. The need for extraoperative ECoG was determined by a multidisciplinary conference of neurologists, neurosurgeons, radiologists, and neuropsychologists. Patient characteristics are summarized in Table 1.

Electrical Stimulation Mapping

Routine bedside clinical ECS was conducted with each left-sided ECoG patient (n = 15) to determine sites involved in language and motor function (Lüders et al. 1988; Nair et al. 2008; Diehl et al. 2010). Right-sided, non-dominant patients were not mapped (Leonard et al. Forthcoming). ECS was performed by an epileptologist only after the seizure focus had been adequately determined and after patients had resumed antiepileptic medication. Stimuli were delivered at 50 Hz, with 2 s trains of 500 μs wide pulses. The delivered current ranged from 2 to 10 mA.

Recordings

Electrophysiological recordings were acquired at a 3051.8 Hz sampling rate with a PZ2 amplifier and RZ2 digital acquisition system (Tucker-Davis Technologies; Alachua, FL, USA) while the patients were quietly resting with eyes open. Sessions lasted 2.3 ± 1.3 min (range 1.0–5.2 min).

Signals were digitally re-referenced to the common median (the common median is more robust than the common average when confronted with artifacts and noisy channels) (Rolston et al. 2009), and notch filtered at 60, 120, and 180 Hz to reduce line noise and its harmonics. For connectivity analysis, the signals were then band-pass filtered from 1 to 100 Hz, and downsampled 15 × to 203.5 Hz. For evoked activity analysis, the signals were band-pass filtered from 1 to 200 Hz and downsampled 7× to 436.0 Hz. Electrodes with clear artifact or epileptiform activity were discarded from analysis before common median referencing.

Table 1 Patient characteristics

Characteristic	
Age, years (±SD)	35.5 ± 13.1
Gender	
Female	6 (40)
Male	9 (60)
# Language electrodes	7.7 ± 5.3 (range 1–22)
# Motor electrodes	7.0 ± 5.4 (range 0–16)
# Cleared electrodes	21.7 ± 8.5 (range 8–36)

Language Network Determination

Two tasks were attempted with each patient, though not every patient completed both: 1) Passive listening to a corpus of short sentences (Texas Instruments/Massachusetts Institute of Technology (TIMIT) database: 2–4 s duration, 16 kHz sampling rate); 2) Repetition of consonant-vowel (CV) syllables (/ba/, /da/, /ga/, /pa/, /ta/, /ka/, /ʃa/, /sa/). The CVs were presented in random order by a male voice unknown to the patients.

For passive listening analysis, evoked responses were manually time-locked to the onset of the sentences. For the CV analysis, evoked responses were time-locked to the onset of the subject's speech.

Evoked spectrograms were generated using Gaussian filters with logarithmically increasing center frequencies and semi-logarithmically increasing bandwidths (1.2–144.0 Hz), and taking the Hilbert transform to obtain the analytic amplitude, as previously described (Canolty et al. 2007; Bouchard et al. 2013). Bootstrapping was used to determine significant time-frequency points within each spectrogram (Canolty et al. 2007). Briefly, surrogate data was generated by randomly shuffling the stimulus onsets 1000 times, creating 1000 pseudo-experiments. Generating spectrograms for each pseudo-experiment provides an estimate of the background distribution of analytic amplitudes for each point of the time-frequency spectrogram. The true experimental spectrograms were then Z-scored against this distribution and a false discovery rate (FDR) of q = 0.01 used to select significant points (Benjamini and Hochberg 1995; Canolty et al. 2007). We further specified that significant electrodes must have significant time-frequency points spanning ≥2 center frequencies and lasting ≥20 ms.

Any electrode showing significant modulations of spectral activity following passive listening or active repetition (as described above) was declared part of the language network (Supplemental Fig. 1).

Functional Connectivity

To estimate functional connectivity, we used imaginary coherence in the alpha band (8–15 Hz) (Hinkley et al. 2011; Englot et al. 2015). Alpha activity peaks during the quiet, resting state, and has excellent retest reliability compared to other frequency bands (Hinkley et al. 2011). In addition, other frequency bands were tested (theta, 4–7 Hz; beta 16–32 Hz; gamma 32–50 Hz).

Coherence was estimated using Thomson's multi-taper method with a time-frequency bandwidth of 3 (unitless parameter), 1 s window, and 5 tapers (Percival and Walden 1993; Mitra and Bokil 2007). The absolute value of the imaginary component was averaged across the alpha frequency band, and normalized with Fisher's Z-transform to produce IC_{xy}, a single value for each pair of electrodes x and y (Fisher 1915; Nolte et al. 2004). When the real component of coherence is removed,

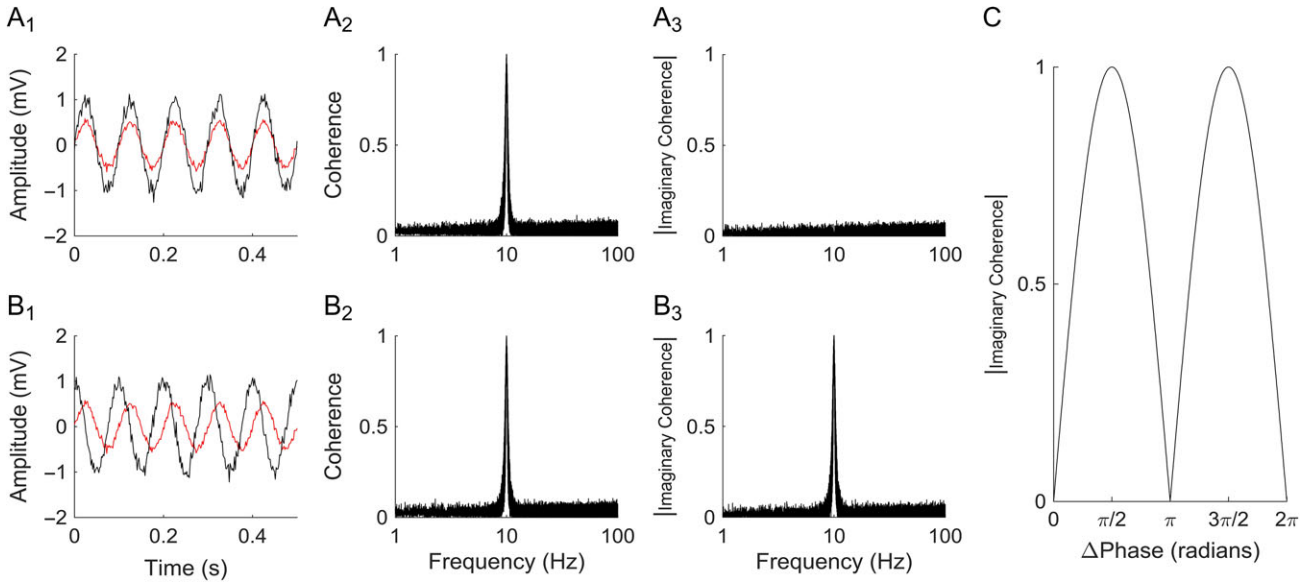

Figure 1. Example of imaginary coherence. (*A1*) Example of volume conduction or common-mode noise. Two 10 Hz sine waves of different amplitudes (red and black traces) with additive random noise are shown. The 2 curves have a 0° phase difference, as might be seen with volume conduction or common-mode noise. (*A2*) The coherence of these 2 sine waves at 10 Hz is 1, while it is near zero at all other frequencies. This is robust to differences in relative signal amplitudes, one of the advantages of coherence analysis. (*A3*) The absolute value of the imaginary coherence, unlike regular coherence, has no peak at 10 Hz, since the 2 signals are in phase (i.e., there is no imaginary or phase component to the coherence). (*B1*) Example of phase-locked signals: two 10 Hz sine waves with additive random noise (red and black) with a fixed 90° phase relationship and different amplitudes. (*B2*) The coherence at 10 Hz is identical to that of *A2*, despite changes in amplitude and phase. (*B3*) However, the absolute value of the imaginary coherence at 10 Hz for these signals is 1, since they have a fixed, non-zero phase difference, likely reflective of a neural signal. (*C*) Imaginary coherence as a function of the phase difference between 2 arbitrary signals is shown. The imaginary coherence is zero when the 2 signals are exactly in phase or 180° out of phase, as might be seen with volume conduction or a shared reference. Imaginary coherence thereby reduces the probability of picking up spurious, non-physiological correlations. Coherence (and imaginary coherence) are robust to differences in signal amplitude, as shown by the sample signals in *A1* and *B1*.

simultaneous (zero time lag) signals are ignored, in favor of signals with set phase differences. This minimizes the contribution of volume conduction and common references to estimates of connectivity, and is less likely to capture erroneous associations (Nolte et al. 2004; Guggisberg et al. 2008). Furthermore, coherence is robust to differences in baseline signal amplitude, reducing sensitivity to differences in electrode impedance and noise. Figure 1 provides additional explanation of the imaginary coherence methodology.

For each electrode x, the median *Z*-transformed imaginary coherence, M_x, was obtained between *x* and all other electrodes *y*: $M_x = \text{median}(IC_{xy})$, where $x \neq y$. This produced a single value estimating how strongly electrode *x* was connected to other electrodes within the network.

Using the nonparametric Wilcoxon rank-sum test, the set of median coherences, M_x, for all sites identified as critical for language was compared to those cleared for language by ECS. The median coherence was used instead of the mean coherence to minimize the influence of potential outlier values. Additionally, the coherence across anatomical regions was compared with an analysis of variance (ANOVA) test followed by post hoc Scheffé test to correct for multiple comparisons.

To determine a baseline value for significance of imaginary coherence, we created surrogate data by computing imaginary coherence matrices as above, but reversing the time-course of one channel for each pairwise comparison. That is, instead of computing the imaginary coherence between $x(t)$ and $y(t)$, we computed the imaginary coherence between $x(t)$ and $y(-t)$. This preserves amplitude and spectral data for both channels, but removes time-varying correlations. A significance threshold was determined as the 95th percentile of these values. The number of significant edges (where the imaginary coherence value exceeded this 95th percentile) was calculated for each electrode, and the number of significant connections compared between language and cleared electrodes.

The root-mean-square (RMS) amplitude of electrode *x* was calculated as an estimate of overall signal amplitude, which is a function of electrode impedance:

$$\text{RMS}_x = \sqrt{\frac{1}{T}\sum_{t=1}^{T}|x(t)|^2},$$

where $x(t)$ is the electrode voltage signal over time and *T* is the total number of samples. Linear regression was used to correlate RMS with electrode imaginary coherence values.

Agglomerative hierarchical clustering was used on the functional connectivity matrix for each patient to determine patterns relating to anatomical or functional relationships. The distance measure was defined as $d_{xy} = 1–IC_{xy}$ (perfect coherence would correspond to $d_{xy} = 0$, while no coherence will correspond to $d_{xy} = 1$). Clusters were formed by joining electrode pairs with the lowest distance, linking these pairs, and then repeating. New clusters use the shortest distance of member electrodes to determine their distance to other clusters or electrodes.

Results

Using imaginary coherence in the alpha band (8–15 Hz), maps of resting-state connectivity were generated from 15 patients with left-sided ECoG grids implanted for epilepsy monitoring. Routine clinical ECS was used to identify electrodes with

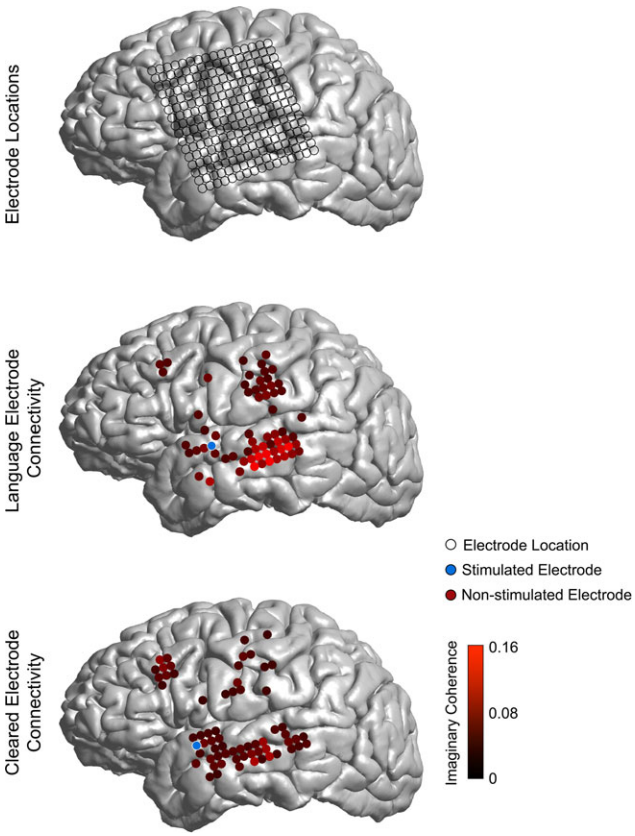

Figure 2. Example of connectivity for language and cleared sites. Top panel: electrode locations for a 256-channel high-density ECoG grid. Middle panel: connectivity between a language site as confirmed by ECS (shown in blue) and all other sites (only top 25% of connections with the language site are shown for clarity). Bottom panel: connectivity between a site confirmed as cleared by ECS (shown in blue) and other sites (top 25% connections with the cleared site are shown for clarity). Note the increased local connectivity between the language site, as compared to the cleared site.

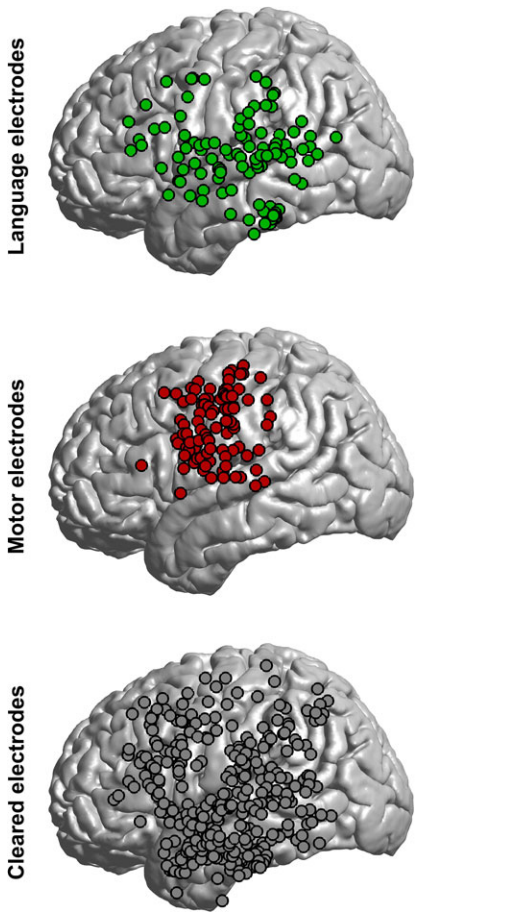

Figure 3. Anatomical locations of electrodes. Electrode locations were co-registered and projected to a common brain. The proportion of language and cleared electrodes was similar across anatomical regions. Warping electrode locations to a standard brain introduces some errors (e.g., motor electrodes over the superior temporal gyrus, which were actually in the pre-, post-, or subcentral gyrus).

language function, motor function, and no function ("clinically cleared"). Examples of connectivity maps for language and cleared electrodes are shown in Figure 2.

Across the 15 patients, ECS identified 115 electrodes as critical for language (7.7 ± 5.3 per patient), 105 for motor (7.0 ± 5.4 per patient), and cleared 326 electrodes (21.7 ± 8.5 per patient). The location of electrodes was consistent with prior reports, with language sites identified in the frontal lobe (primarily the frontal operculum and precentral gyrus), temporal lobe (inferior, middle, and superior gyri), and parietal lobe (postcentral gyrus and supramaginal gyrus; Fig. 3) (Penfield and Erickson 1941; Penfield and Jasper 1954; Berger et al. 1989; Ojemann et al. 1989; Ojemann 1993; Chang et al. 2017). Cleared sites occurred in roughly the same proportions as language sites across anatomical regions, though motor sites were concentrated in the pre- and postcentral gyri (Fig. 3).

As hypothesized, the imaginary coherence between identified language electrodes and other electrodes was significantly higher when compared to cleared electrodes ($P = 0.001$, rank-sum test; Fig. 4A). The increased coherence was not an isolated finding in a single frequency band, and also held for the neighboring theta ($P = 0.002$) and beta ($P = 0.003$) bands. Moreover, the increased connectivity persisted during language tasks, and was not restricted to resting networks ($P = 0.001$; Fig. 4A). Controlling for anatomical region did not affect these sites, as functional connectivity was always greater among language sites than cleared sites regardless of region analyzed (Supplemental Fig. 2; ANOVA, $F = 5.7$, $P < 0.001$). Additionally, functional connectivity did not correlate with electrode RMS amplitude (adjusted $R^2 = 0.0047$; Supplemental Fig. 3), which is a measure of signal amplitude and a function of electrode impedance, nor did electrode RMS significantly differ between language and cleared electrodes (36.2 ± 24.4 vs. 39.9 ± 23.2; $P = 0.16$).

As a further test, we used surrogate, time-reversed data to compute a 95% significance threshold for imaginary coherence for each patient (see Materials and Methods). Time-reversed data preserve amplitude and frequency content, but remove time-varying correlations. Using this method, language electrodes had significantly more connections than cleared electrodes ($P < 0.005$). This also held if the significance threshold was raised to 99% ($P = 0.001$) or 99.9% ($P = 0.002$).

We further restricted this analysis to electrodes involved in functional language networks, as defined by significant modulations in evoked local field potentials (LFPs) in response to passive listening or active repetition tasks (see Materials and Methods, Supplemental Fig. 1). Of note, many clinically cleared electrodes showed significant evoked LFP responses (67.1%) and many electrodes that mapped positively for language showed

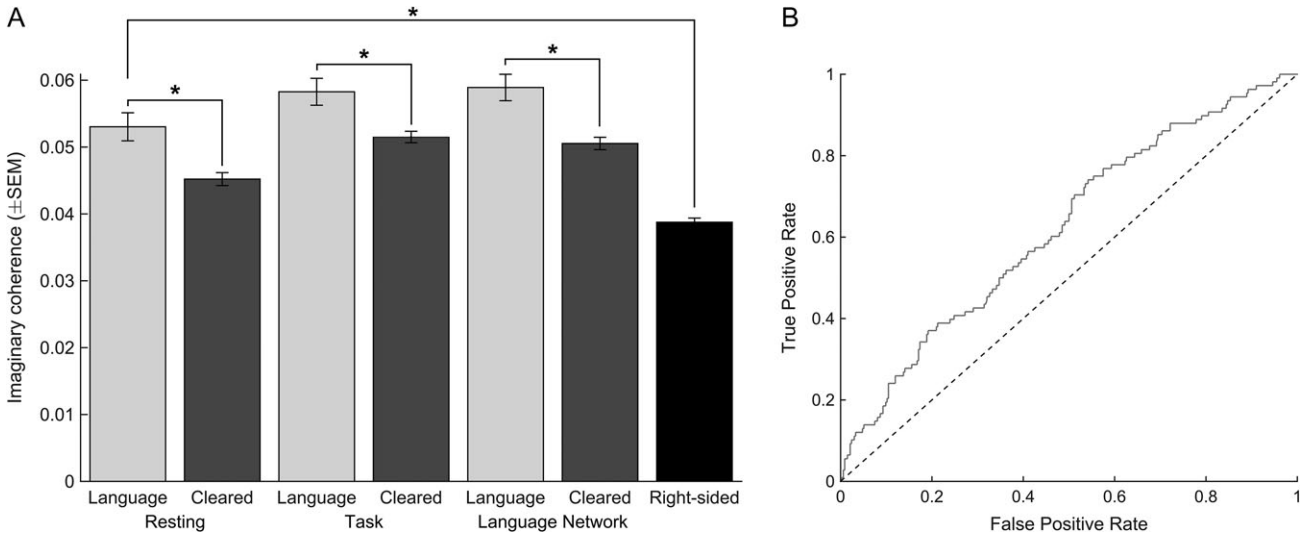

Figure 4. Connectivity of language sites is higher than cleared or right-sided, non-dominant sites. (*A*) The median alpha band imaginary coherence of language sites (from left-sided, dominant hemispheres) was significantly higher than cleared sites in the same patients, and also higher than electrodes from non-dominant right-sided ECoG grids (non-dominant hemispheres are presumed to not have language sites). This was true when coherence was calculated during quiet rest ("Resting", 2 leftmost bars), during language tasks ("Task"; middle 2 bars), or when the analysis was restricted to electrodes with significant local field potential modulations in response to language tasks ("Language Network", right-sided bars). (*B*) Receiver operating characteristic (ROC) curve showing the rate of true positives and false positives as a function of a dynamic threshold of imaginary coherence.

no evoked response (21.2%; Supplemental Fig. 1). Even when functional connectivity analyses were restricted to these functionally defined language networks, ESC-defined language sites still had significantly higher connectivity than ESC-cleared sites ($P = 0.0002$; Fig. 4A).

This relationship continued to hold when comparing language electrodes to electrodes from patients with non-dominant (right-sided) ECoG grids, where electrodes are presumed clinically cleared by virtue of their location in the non-dominant hemisphere (Fig. 4A). This was true whether all right-side ECoG electrodes were used ($P = 2.2 \times 10^{-11}$), only those in the temporal lobe ($P = 6.8 \times 10^{-9}$), or if only homologous sites were used ($P = 2.9 \times 10^{-11}$). For homologous sites, all electrodes were first transformed to common MNI space. All right-sided electrodes that were within 4 mm (the pitch of our ECoG arrays) of a mirrored language electrode were used. This resulted in 129 homologous right-sided electrodes, with a mean distance of 3.4 ± 0.6 mm (range 0.6–4.0) from language electrodes mirrored from the left to right side. Significant differences were also obtained when using homologous sites within 2 or 6 mm, as well (data not shown).

While the connectivity of language sites was overall significantly higher than cleared sites, these distributions had a high degree of overlap, as illustrated in a receiver operating characteristic (ROC) curve (Fig. 4B).

To test whether this was a specific property of language electrodes, we also analyzed connectivity as it related to electrodes with identified motor function. This produced similar results, with significant differences in the theta ($P = 0.015$) and alpha bands ($P = 0.022$; Fig. 5).

Agglomerative hierarchical clustering was used on each patient to identify patterns within the generated functional connectivity matrices (see Materials and Methods). Clusters determined through this method appeared largely dominated by anatomical region, rather than relating to the language/cleared category (Supplemental Fig. 4).

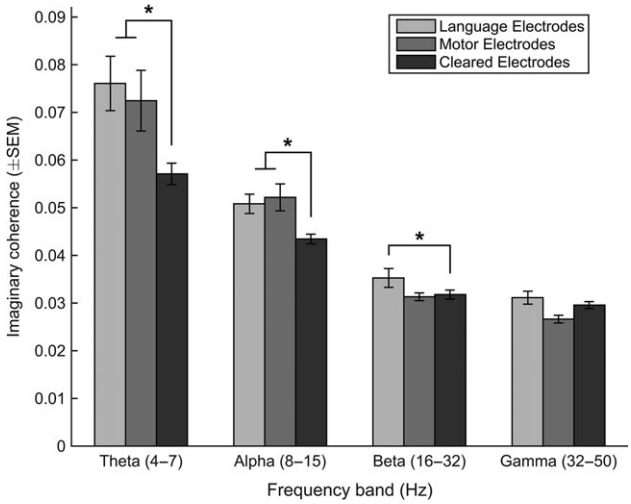

Figure 5. Connectivity as a function of frequency band. Median imaginary coherence is shown for each tested frequency band. Significant differences were found between language and cleared electrodes at all frequencies and between motor and cleared electrodes for theta and alpha frequency bands.

Discussion

What makes critical language sites, as determined by ECS, unique? One hypothesis is that these sites are strongly connected to nearby cortex. Disruption of their activity with ECS would be therefore more likely to propagate throughout this network, and more likely to lead to speech arrest, anomia, or other signs of transient dysfunction of the language system. Alternatively, their increased connectivity might be a sign of their central role in language networks, and their disruption by ECS (even if it were not to spread) would lead to overt deficits.

We tested the hypothesis that language sites are more strongly connected than cleared (negative) sites by analyzing functional connectivity across 15 patients undergoing chronic left-sided ECoG recording and bedside ECS for epilepsy surgery, along with 4 patients undergoing right-sided ECoG. As hypothesized, language sites showed higher alpha band (8–15 Hz) imaginary coherence (a reliable estimate of functional connectivity; see Materials and Methods and Fig. 1) than sites cleared by electrical stimulation. This also held true for neighboring frequency bands, suggesting that this finding is robust to precise frequency band specifications (Fig. 5). Furthermore, language sites had higher connectivity than sites in right-sided ECoG grids, which is expected since the non-dominant lobe lacks critical language sites for anomia and repetition by ECS (Ojemann et al. 1989; Ojemann 1991; Chang et al. 2017; Leonard et al. Forthcoming) (Fig. 4).

These findings of increased connectivity are consistent with prior studies of functional connectivity. Using resting-state EEG, Nicolo et al. showed that increased imaginary coherence of language sites correlated with the degree of language improvement post-stroke (Nicolo et al. 2015). Using resting-state MEG, Martino et al. showed that increased imaginary coherence predicted eloquent regions as determined be intraoperative stimulation mapping (Martino, Honma, et al. 2011). Tarapore et al. further showed (again with resting-state MEG) that increased imaginary coherence of language regions near brain tumors predicted poor language outcomes when these tumors were resected (Tarapore et al. 2012).

The imaginary coherence values observed above are far lower than those expected from conventional coherence analysis. Given this low amplitude, are these values still significant? While none of the studies in the preceding paragraph report raw coherence values (Martino, Honma, et al. 2011; Tarapore et al. 2012; Nicolo et al. 2015), our results are similar or higher than those reported in other studies using imaginary coherence for human data (Meziane et al. 2015; Fujimoto et al. 2016; Ohki et al. 2016). We further sought to validate this by determining a significance threshold from surrogate data. Using time-reversed versions of our ECoG data (which shares all amplitude and spectral properties, but removes time-varying correlations; see Materials and Methods), we found a 95% significance threshold of 0.0480, which is lower than our reported imaginary coherence values. Lastly, when pruning connectivity networks by this threshold, we found significantly more connections from language electrodes than cleared electrodes (see Results).

The hypothesis that increased connectivity is a factor in ECS is not limited to language sites. That is, evoked activity is more likely to produce overt responses if it spreads to a greater area of cortex, and increased functional connectivity may encourage this spreading. This may be true for any effect of ECS, not just language. To test this, we also examined functional connectivity for motor sites (where ECS evokes a motor response). Again, connectivity was higher in motor sites than cleared sites, as was the case for language sites (Fig. 3).

Clustering analysis of the raw functional connectivity matrices for each patient was dominated by anatomical relationships, rather than membership in the ESM language/cleared category (Supplemental Fig. 4). This is likely due in part to the heterogeneous location of language sites (found within temporal, frontal, and parietal lobes) and cleared sites. Our finding, that the median connectivity values are higher for language electrodes than cleared electrodes, might therefore be explained as a heightened tendency toward higher connectivity for language sites across the observed cortex, rather than increased connectivity with precisely defined regions. However, more nuanced recording and clustering methods might discern such relationships.

While the increased connectivity was significant across the population of tested electrodes, the distributions of connectivity between language and cleared sites had a large degree of overlap. That is, some cleared electrodes had higher measures of connectivity than the least-connected language electrodes (Fig. 4B). Thus, there are clearly additional factors that determine whether a site is critical for language than functional connectivity. Additional factors like more whole-brain measures of connectivity (e.g., fMRI and MEG (Englot et al. 2016)) and anatomical information (e.g., from DTI (Skudlarski et al. 2008)) might be necessary to create a more predictive model.

Limitations of the above analyses are those common to ECoG recordings. The subjects have medically refractory epilepsy and are on antiepileptic medications; they therefore might have differing physiology than patients without epilepsy or patients with other neurological disorders. While many studies of language neurophysiology have been fruitfully conducted with these patients (Mesgarani and Chang 2012; Bouchard et al. 2013; Hullett et al. 2016), these concerns remain. However, even if our conclusions were only applicable to patients with epilepsy, it is these patients who undergo bedside ECS. A better understanding of ECS may lead to safer surgeries for this particular patient group, even if the conclusions are not generalizable.

Another limitation is the interpretation of functional connectivity. Metrics of functional connectivity measure comodulation in different ways, but are never able to conclusively differentiate a shared driving source from mutual influence (Bastos and Schoffelen 2015). Such differentiation requires other means, such as postmortem fiber tracing, diffusion tractography, or the measurement of cortico-cortical evoked potentials (Catani et al. 2005; Conner et al. 2011; Martino, De Witt Hamer, et al. 2011; Keller, Honey, Entz, et al. 2014; Keller, Honey, Mégevand, et al. 2014; Enatsu et al. 2016).

A further confounder is the limited extent of ECoG recordings, as compared to global sampling of the brain by magnetoencephalography (MEG) or functional magnetic resonance imaging (fMRI). ECoG measures of connectivity, when using grids, are predisposed toward identifying local connections, and are generally incapable of identifying long range connections. Again, the difference in measured connectivity between language, motor, and cleared sites might therefore indicate tighter local networks for these critical sites versus wider distributed networks for "cleared" sites. However, prior studies using EEG and MEG, capturing the whole brain, have found that anatomical language areas have increased connectivity as determined by imaginary coherence, suggesting that our findings are not limited by the spatial extent of ECoG grids (Martino, Honma, et al. 2011; Tarapore et al. 2012; Nicolo et al. 2015).

We appreciate that the observed functional coherence patterns do not map to anatomical or task-related localizations at this level of analysis. A more complete understanding of how critical language sites are localized will likely require more detailed anatomical studies (e.g., high-resolution tractography), additional means of determining effective connectivity (e.g., cortico-cortical evoked potentials (Kunieda et al. 2015)), and an improved understanding of normal language processing (i.e., what are these critical language sites doing during normal speech acts as compared to non-critical sites?). Such additional research projects will provide invaluable additional lenses with which to view the phenomenon of language mapping with electrical stimulation.

Conclusion

Critical language sites, as determined by ECS, show greater resting-state connectivity than cleared sites. This is consistent with the hypothesis that critical language sites are highly connected within the local cortical network, perhaps explaining why their disruption with ECS leads to transient disturbances in language function.

Supplementary Material

Supplementary data are available at *Cerebral Cortex* online.

Funding

J.D.R. was supported by a fellowship from the National Institute on Deafness and Other Communication Disorders (1F32DC013 953-01).

Notes

The authors wish to thank Morgan Lee for assistance with brain reconstructions. *Conflict of Interest*: None declared.

References

Bastos AM, Schoffelen J-M. 2015. A tutorial review of functional connectivity analysis methods and their interpretational pitfalls. Front Syst Neurosci. 9:175.

Benjamini Y, Hochberg Y. 1995. Controlling the false discovery rate—a practical and powerful approach to multiple testing. J R Stat Soc Ser B-Methodol. 57:289–300.

Berger MS, Kincaid J, Ojemann GA, Lettich E. 1989. Brain mapping techniques to maximize resection, safety, and seizure control in children with brain tumors. Neurosurgery. 25: 786–792.

Bouchard KE, Mesgarani N, Johnson K, Chang EF. 2013. Functional organization of human sensorimotor cortex for speech articulation. Nature. 495:327–332.

Canolty RT, Soltani M, Dalal SS, Edwards E, Dronkers NF, Nagarajan SS, Kirsch HE, Barbaro NM, Knight RT. 2007. Spatiotemporal dynamics of word processing in the human brain. Front Neurosci. 1:185–196.

Catani M, Jones DK, ffytche DH. 2005. Perisylvian language networks of the human brain. Ann Neurol. 57:8–16.

Chang EF, Breshears JD, Raygor KP, Lau D, Molinaro AM, Berger MS. 2017. Stereotactic probability and variability of speech arrest and anomia sites during stimulation mapping of the language dominant hemisphere. J Neurosurg. 126(1):114–121.

Conner CR, Ellmore TM, DiSano MA, Pieters TA, Potter AW, Tandon N. 2011. Anatomic and electro-physiologic connectivity of the language system: a combined DTI-CCEP study. Comput Biol Med. 41:1100–1109.

Diehl B, Piao Z, Tkach J, Busch RM, LaPresto E, Najm I, Bingaman B, Duncan J, Lüders H. 2010. Cortical stimulation for language mapping in focal epilepsy: correlations with tractography of the arcuate fasciculus. Epilepsia. 51:639–646.

Enatsu R, Gonzalez Martinez J, Bulacio J, Mosher JC, Burgess RC, Najm I, Nair DR. 2016. Connectivity of the frontal and anterior insular network: a cortico-cortical evoked potential study. J Neurosurg. 125(1):90–101.

Englot DJ, Hinkley LB, Kort NS, Imber BS, Mizuiri D, Honma SM, Findlay AM, Garrett C, Cheung PL, Mantle M, et al. 2015. Global and regional functional connectivity maps of neural oscillations in focal epilepsy. Brain. 138:2249–2262.

Englot DJ, Konrad PE, Morgan VL. 2016. Regional and global connectivity disturbances in focal epilepsy, related neurocognitive sequelae, and potential mechanistic underpinnings. Epilepsia. 57:1546–1557.

Findlay AM, Ambrose JB, Cahn Weiner DA, Houde JF, Honma S, Hinkley LBN, Berger MS, Nagarajan SS, Kirsch HE. 2012. Dynamics of hemispheric dominance for language assessed by magnetoencephalographic imaging. Ann Neurol. 71:668–686.

Fisher RA. 1915. Frequency distribution of the values of the correlation coefficient in samples from an indefinitely large population. Biometrika. 10:507.

Foster BL, He BJ, Honey CJ, Jerbi K, Maier A, Saalmann YB. 2016. Spontaneous neural dynamics and multi-scale network organization. Front Syst Neurosci. 10:7.

Fujimoto T, Okumura E, Kodabashi A, Takeuchi K, Otsubo T, Nakamura K, Yatsushiro K, Sekine M, Kamiya S, Shimooki S, et al. 2016. Sex differences in gamma band functional connectivity between the frontal lobe and cortical areas during an auditory oddball task, as revealed by imaginary coherence assessment. Open Neuroimag J. 10:85–101.

Guggisberg AG, Honma SM, Findlay AM, Dalal SS, Kirsch HE, Berger MS, Nagarajan SS. 2008. Mapping functional connectivity in patients with brain lesions. Ann Neurol. 63:193–203.

Herman AB, Houde JF, Vinogradov S, Nagarajan SS. 2013. Parsing the phonological loop: activation timing in the dorsal speech stream determines accuracy in speech reproduction. J Neurosci. 33:5439–5453.

Hinkley LBN, Vinogradov S, Guggisberg AG, Fisher M, Findlay AM, Nagarajan SS. 2011. Clinical symptoms and alpha band resting-state functional connectivity imaging in patients with schizophrenia: implications for novel approaches to treatment. Biol Psychiatry. 70:1134–1142.

Hullett PW, Hamilton LS, Mesgarani N, Schreiner CE, Chang EF. 2016. Human superior temporal gyrus organization of spectrotemporal modulation tuning derived from speech stimuli. J Neurosci. 36:2014–2026.

Keller CJ, Honey CJ, Entz L, Bickel S, Groppe DM, Toth E, Ulbert I, Lado FA, Mehta AD. 2014. Corticocortical evoked potentials reveal projectors and integrators in human brain networks. J Neurosci. 34:9152–9163.

Keller CJ, Honey CJ, Mégevand P, Entz L, Ulbert I, Mehta AD. 2014. Mapping human brain networks with cortico-cortical evoked potentials. Philos Trans R Soc Lond, B, Biol Sci. 369: 20130528–20130528.

Kunieda T, Yamao Y, Kikuchi T, Matsumoto R. 2015. New approach for exploring cerebral functional connectivity: review of cortico-cortical evoked potential. Neurol Med Chir (Tokyo). 55:374–382.

Leonard MK, Cai R, Babiak MC, Ren A, Chang EF. Forthcoming. The peri-Sylvian cortical networks underlying single word repetition revealed by electrocortical stimulation and direct neural recordings. Brain Lang. doi: 10.1016/j.bandl.2016.06.001. [Epub ahead of print]

Lüders H, Lesser RP, Dinner DS, Morris HH. 1988. Localization of cortical function: new information from extraoperative monitoring of patients with epilepsy. Epilepsia. 29:S56–S65.

Martino J, De Witt Hamer PC, Vergani F, Brogna C, de Lucas EM, Vázquez-Barquero A, García-Porrero JA, Duffau H. 2011. Cortex-sparing fiber dissection: an improved method for the study of white matter anatomy in the human brain. J Anat. 219:531–541.

Martino J, Honma SM, Findlay AM, Guggisberg AG, Owen JP, Kirsch HE, Berger MS, Nagarajan SS. 2011. Resting functional connectivity in patients with brain tumors in eloquent areas. Ann Neurol. 69:521–532.

Mesgarani N, Chang EF. 2012. Selective cortical representation of attended speaker in multi-talker speech perception. Nature. 485:233–236.

Meziane HB, Moisello C, Perfetti B, Kvint S, Isaias IU, Quartarone A, Di Rocco A, Ghilardi MF. 2015. Movement preparation and bilateral modulation of beta activity in aging and Parkinson's disease. PLoS ONE. 10:e0114817.

Mitra PP, Bokil H. 2007. Observed brain dynamics. Oxford: Oxford University Press.

Nair DR, Burgess R, McIntyre CC, Lüders H. 2008. Chronic subdural electrodes in the management of epilepsy. Clin Neurophysiol. 119:11–28.

Nicolo P, Rizk S, Magnin C, Di Pietro M, Schnider A, Guggisberg AG. 2015. Coherent neural oscillations predict future motor and language improvement after stroke. Brain. 138:3048–3060.

Nolte G, Bai O, Wheaton L, Mari Z, Vorbach S, Hallett M. 2004. Identifying true brain interaction from EEG data using the imaginary part of coherency. Clin Neurophysiol. 115: 2292–2307.

Ohki T, Gunji A, Takei Y, Takahashi H, Kaneko Y, Kita Y, Hironaga N, Tobimatsu S, Kamio Y, Hanakawa T, et al. 2016. Neural oscillations in the temporal pole for a temporally congruent audio-visual speech detection task. Sci Rep. 6: 37973.

Ojemann G. 2013. Human temporal cortical single neuron activity during language: a review. Brain Sci. 3:627–641.

Ojemann G, Ojemann J, Lettich E, Berger M. 1989. Cortical language localization in left, dominant hemisphere. An electrical stimulation mapping investigation in 117 patients. J Neurosurg. 71:316–326.

Ojemann GA. 1991. Cortical organization of language. J Neurosci. 11:2281–2287.

Ojemann GA. 1993. Functional mapping of cortical language areas in adults. Intraoperative approaches. Adv Neurol. 63: 155–163.

Penfield W, Erickson TC 1941. Epilepsy and cerebral localization.

Penfield W, Jasper HH. 1954. Epilepsy and the functional anatomy of the human brain. Boston, MA: Little Brown.

Percival DB, Walden AT. 1993. Spectral analysis for physical applications. Cambridge, England: Cambridge University Press.

Rolston JD, Gross RE, Potter SM. 2009. Common median referencing for improved action potential detection with multielectrode arrays. Conf Proc IEEE Eng Med Biol Soc. 2009:1604–1607.

Sanai N, Mirzadeh Z, Berger MS. 2008. Functional outcome after language mapping for glioma resection. N Engl J Med. 358: 18–27.

Skudlarski P, Jagannathan K, Calhoun VD, Hampson M, Skudlarska BA, Pearlson G. 2008. Measuring brain connectivity: diffusion tensor imaging validates resting state temporal correlations. Neuroimage. 43:554–561.

Swanson SJ, Sabsevitz DS, Hammeke TA, Binder JR. 2007. Functional magnetic resonance imaging of language in epilepsy. Neuropsychol Rev. 17:491–504.

Tarapore PE, Martino J, Guggisberg AG, Owen J, Honma SM, Findlay A, Berger MS, Kirsch HE, Nagarajan SS. 2012. Magnetoencephalographic imaging of resting-state functional connectivity predicts postsurgical neurological outcome in brain gliomas. Neurosurgery. 71:1012–1022.

Yang T, Hakimian S, Schwartz TH. 2014. Intraoperative ElectroCorticoGraphy (ECog): indications, techniques, and utility in epilepsy surgery. Epileptic Disord. 16:271–279.